Coordination Chemistry Reviews, 111 (1991) 83–90
Elsevier Science Publishers B.V., Amsterdam

Intramolecular energy transfer in polyoxometaloeuropate lattices and their application to a.c. electroluminescence device

Toshihiro Yamase* and Haruo Naruke

Research Laboratory of Resources Utilization
Tokyo Institute of Technology, 4259 Nagatsuta, Midori-ku,
Yokohama 227, Japan

Abstract

Crystal Structures of four polyoxometaloeuropates, $Na_9[EuW_{10}O_{36}].32H_2O$ (1), $K_{15}H_3[Eu_3(H_2O)_3(SbW_9O_{33})(W_5O_{18})_3].25.5H_2O$ (2), $[NH_4]_{12}H_2[Eu_4(H_2O)_{16}(MoO_4)(Mo_7O_{24})_4].13H_2O$ (3), and $Eu_2(H_2O)_{12}[Mo_8O_{27}].6H_2O$ (4) are investigated to understand the relaxation process of the oxygen-to-metal (O→M) charge-transfer excitation energy in the polyoxometalate lattice.

The temperature dependence of the intramolecular energy transfer from the O→M LMCT states to Eu^{3+} in the polyoxometaloeuropate lattices indicates that the M-O-M and Eu-O-M bond angles of about 150° allow the hopping of d^1 electron among MO_6 octahedra and to EuO_8 (or EuO_9) site to be the deactivation of the O→M LMCT state due to the deactivated recombination between the electron and hole in the lattice. Co-ordination of aqua ligands to Eu^{3+} leads to a decrease in lifetime of the emitting state of $^5D_0$, due to the vibronic coupling of the $^5D_0$ state with the vibrational states of high frequency OH oscillators.

Dispersion-typed electroluminescence (EL) cell is constructed with a highly photoluminescent $[EuW_{10}O_{36}]^{9-}$ system. With a.c. excitation to the divice consisting of the doublet structure of emissive $[EuW_{10}O_{36}]^{9-}$ and insulating Mylar film layers, the $[EuW_{10}O_{36}]^{9-}$ layer exhibits EL which matches the photoluminescence spectrum of the solid. A multicolor display in combination with other polyoxometalolanthanoates is possible.

1. INTRODUCTION

The polyoxometalolanthanoate, constituting a great variety of composition and structure, can be regarded as molecular fragments of an infinite metal oxide doped with lanthanide elements. The photoexcitation into the oxygen-to-metal (O→M) ligand-to-metal charge transfer (LMCT) bands of polyoxometaloeuropates leads to an intramolecular energy transfer from

polyoxometalate ligands to Eu^{3+}. This behavior has been investigated for several polyoxotungstoeuropates such as $Na_9[Eu(W_5O_{18})_2].18H_2O$, $K_{13}[Eu(SiW_{11}O_{39})_2].20H_2O$, $K_{17}[Eu(P_2W_{17}O_{61})_2].48H_2O$, and $K_{15}H_3[Eu_3(H_2O)_3(SbW_9O_{33})(W_5O_{18})_3].25.5H_2O$ [1-5]. The efficiency of the intramolecular energy transfer strongly depends on the structure of the polyoxotungstate ligands, as demonstrated by a photoluminescence study of the last complex [5]. Although the detail of the crystal structure is essential for a better understanding of the luminescence properties, only polyoxometaloeuropates of known crystal structure are $Na_9[EuW_{10}O_{36}].32H_2O$ (1), $K_{15}H_3[Eu_3(H_2O)_3(SbW_9O_{33})(W_5O_{18})_3].25.5H_2O$ (2), $[NH_4]_{12}H_2[Eu_4(H_2O)_{16}(MoO_4)(Mo_7O_{24})_4].13H_2O$ (3), and $Eu_2(H_2O)_{12}[Mo_8O_{27}].6H_2O$ (4), which have been characterized by x-ray crystallography [5-8]. In the present study, our interest is focussed on the intramolecular energy transfer in the above four polyoxometaloeuropate lattices. Also, of interest is the description of the a.c.-drived powder-typed electroluminescence (EL) cell based on the polyoxometalolanthanoate.

2. EXPERIMENTAL

Polyoxometaloeuropates, (1)-(4), were prepared and their crystal structures were determined as previously [5-8]. The details of the crystal data are given in Table 1.

Table 1
Crystallographic data for (1)-(4)

	(1)	(2)	(3)	(4)
Space group	Cc	C2/m	C2/c	$P\bar{1}$
a, Å	11.484(5)	30.250(7)	19.539(6)	10.105(3)
b, Å	23.020(6)	18.568(5)	43.31 (1)	12.006(5)
c, Å	23.580(6)	22.101(6)	20.358(6)	9.365(4)
α, deg	90.00	90.00	90.00	122.59(3)
β, deg	91.71(3)	109.19(8)	117.88(2)	90.12(3)
γ, deg	90.00	90.00	90.00	98.33(3)
U, $Å^3$	6231(3)	11723(5)	15229(8)	942.8(7)
Z	4	4	4	1
$R(F_0)$	0.070	0.125	0.065	0.063
$R_w(F_0)$	0.086	0.164	0.080	0.109

The electroluminescent $[EuW_{10}O_{36}]^{9-}$ layer was fabricated as powder of the water-insoluble alkaline-earth metal salt of $[EuW_{10}O_{36}]^{9-}$, which was deposited on the transparent SnO_2/In_2O_3 (ITO) electrode placed on the flat bottom of the glass vessel containing the aqueous solution of (1) and $CaCl_2$ and dried in the air after taking the electrode out of the

mixed solution. A Mylar film with 4-12 μm thickness was put on the $[EuW_{10}O_{36}]^{9-}$ layer as an insulating layer and covered with another ITO electrode to sandwich the luminescent $[EuW_{10}O_{36}]^{9-}$ layer. A spring clip was loaded between the two ITO electrodes to assist the mechanical tightness.

3. RESULTS AND DISCUSSION

3.1 Structure of anions

The representation of the four anions as an assembly of linked MO_6 octahedra is shown in Figure 1.

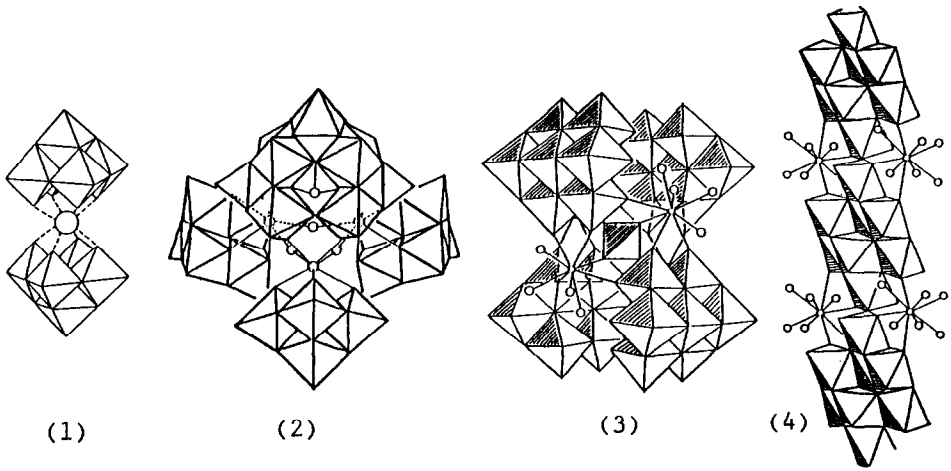

Figure 1. Four representative anion structures of polyoxometaloeuropates (1)-(4) in polyhedral notation.

W_5O_{18} group of the half anion in (1) is derived from the edge-shared WO_6 octahedral $[W_6O_{19}]^{2-}$ by removal of one tungsten atom and its unshared oxygen atom. Four oxygen atoms formerly bonded to the missing tungsten atom are bonded to the Eu atom, leading to the eight-fold co-ordination of Eu^{3+}. The anion has approximately D_4 point-symmetry [6]. There is no aqua ligand co-ordinated to Eu^{3+}.

A central trinuclear $Eu_3(H_2O)_3$ core in the anion of (2) is linked tetrahedrally by three W_5O_{18} groups and one B-α type SbW_9O_{33} group. The anion has approximately C_{3v} point-symmetry [5]. The SbW_9O_{33} group is the trivacant Keggin structured B-α type ligand which contains a three-co-ordinate Sb^{III} and three corner-sharing W_3O_{13} groups (consisting of three edge-shared WO_6 octahedra). Each Eu^{3+} in the $Eu_3(H_2O)_3$ core achieves eightfold co-ordination by attachment of one W_5O_{18} (four oxygens), one SbW_9O_{33} (two oxygens), and two aqua ligands (two oxygens).

The anion in (3) consists of a central $[Eu_4(MoO_4)(H_2O)_{16}]^{10+}$ unit and four edge-shared MoO_6 octahedral Mo_7O_{24} groups, exhibiting an overall point symmetry of D_{2d} [7]. Each of Eu atoms achieves ninefold co-ordination with oxygen atoms: one oxygen atom from the MoO_4 tetrahedron, two oxygen atoms from one Mo_7O_{24} group, two oxygen atoms from other Mo_7O_{24} groups, and four oxygen atoms from four aqua ligands.

The unit in (4) is isostructural to the anion of $[NH_4]_6[Mo_8O_{27}].4H_2O$. Eu^{3+} is linked by six aqua oxygen atoms, two oxygen atoms of Mo_8O_{27} unit, and one oxygen atom belonging to a MoO_6 octahedron of neighboring Mo_8O_{27} unit, resulting in formation of an infinite belt of the octamolybdate $\{[Mo_8O_{27}]^{6-}\}_\infty$ [8].

Figure 2 shows the shape of co-ordination for the Eu atom in the anions and Table 2 summarizes Eu-O and Eu-O_w (aqua O atom) bond distances and Eu-O-M bond angles.

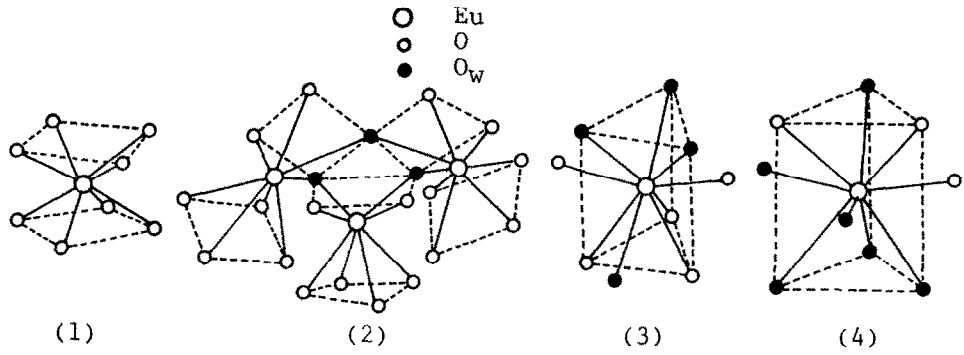

Figure 2. Shapes of co-ordination polyhedra around Eu^{3+} for anions of (1)-(4).

Table 2
Range of Eu-oxygen bond lengths(Å) and Eu-O-M(W or Mo) bond angles (°) for (1)-(4)

	(1)	(2)	(3)	(4)
Eu-O	2.39(3)-2.46(3)	2.28(4)-2.51(3)	2.38(1)-2.48(2)	2.41(1)-2.58(1)
mean	2.43	2.39	2.43	2.46
Eu-O_w	----	2.54(4)-2.64(3)	2.43(2)-2.59(2)	2.43(2)-2.61(1)
mean		2.55	2.49	2.48
Eu-O-M	128(1)-132(1)	122(2)-127(2) 149(2)-153(2)	147(1)-157(8)	147.3(6)-158.4(7)

The local symmetry around Eu^{3+} for the two polyoxotungstoeuropates of (1) and (2) is approximately square antiprismatic, while the one for the two polyoxomolybdoeuropates of (3)

and (4) is approximately tricapped-trigonal prismatic. The mean Eu-O_w distance is longer than the mean Eu-polyoxometalate O atom distance. The Eu-O-M bond angles can be divided into two types: about 130° and about 150°. The complex (2) possesses a distinguishably long mean Eu-O_w distance (2.55 Å) and two types of the Eu-O-M bond angle (122-127° and 149-153°).

3.2 Photoluminescence and intramolecular energy transfer

Photoexcitation of the O→M(W or Mo) LMCT bands of (1)-(4) gives the emission of Eu^{3+}. The emission originates from both $^5D_0$ and $^5D_1$ excited states of Eu^{3+} and the luminescent transitions all terminate in the J=0-4 levels of the ^7F_J ground state. The luminescence intensity of $^5D_1 \rightarrow {}^7F_J$ is very weak, especially for the polyoxotungstoeuropates of (1) and (2). The $^5D_1 \rightarrow {}^7F_4$ transition for (3) and (4) is superimposed in the region of the strong $^5D_0 \rightarrow {}^7F_2$ transition. Figure 3 exemplifies the photoluminescence spectra of (4) at 77K. The spectroscopic detail of the photoluminescence for (4) was previously discussed [8].

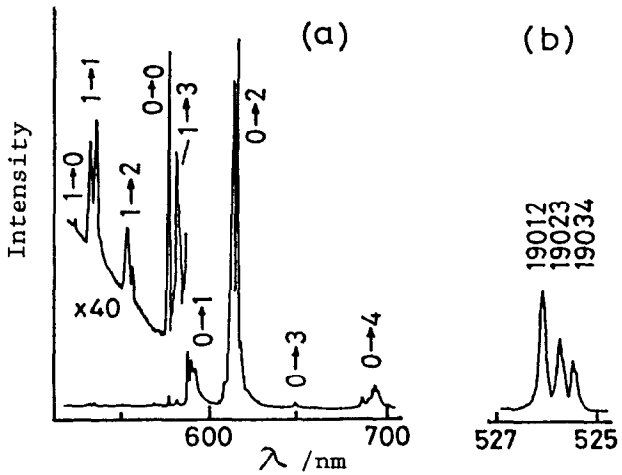

Figure 3. Photoluminescence spectrum of (4) at 77K. Numbers in (a) indicate J→J' for the $^5D_J \rightarrow {}^7F_{J'}$ transitions. The spectrum (b) of the $^5D_1 \rightarrow {}^7F_0$ transition under high resolution shows the position of the emission line in frequency units.

Lifetimes (τ_{CT}) and quantum yields (ϕ_{CT}) of the $^5D_0$ luminescence on the O→M LMCT photoexcitation are listed in Table 3, where τ_{CT} is measured based on exponential decays for the $^5D_0 \rightarrow {}^7F_J$ emission.The intramolecular energy transfer from the O→W LMCT excited states of the polyoxometalate ligands to the emitting $^5D_0$ level is strongly affected by the conformation of the WO_6 octahedra of the ligands, if ϕ_{CT} of (1) is compared with that of (2): the ligands consisting of only edge-sharing WO_6 octahedra with W-O-W bond angles of about 100° give high ϕ_{CT} and a small dependence of ϕ_{CT} on the temperature, while the ligands

involving the corner-sharing WO_6 octahedra with W-O-W bond angles of about 150° via a two-co-ordinate oxygen atom in the conformation (Table 2) give a strong dependence of ϕ_{CT} on the temperature, indicating an increase in ϕ_{CT} with a decrease in the temperature. This has been explained in terms of the thermally activated hopping of the d^1 electron produced by the photoexcitation into the O→M LMCT bands among the corner-sharing MO_6 octahedra [5], which is followed by the deactivated recombination between the electron and hole, with a resultant decrease in the probability of the energy transfer to Eu^{3+} in the lattice.

Table 3
τ_{CT} and ϕ_{CT} of the $^5D_0$ luminescence upon excitation of the O→M LMCT bands for (1)-(4)

	τ_{CT}/ms			ϕ_{CT}		
	temperature/K			temperature/K		
	300	77	4.2	300	77	4.2
(1)	2.8†	3.3†	3.7	0.80†	0.9†	----
(2)	1.1 ± 0.2	1.1 ± 0.2	1.1	0.25	0.51	0.55
(3)	0.20 ± 0.01 (5)*	0.24 ± 0.02 (11)*	---	0.07	0.12	----
(4)	0.17 ± 0.01 (5)*	0.17 ± 0.01 (12)*	0.16 (13)*	0.013 (1 x 10^{-3})*	0.029 (1 x 10^{-3})*	0.034

* τ_{CT} (in μs unit) and ϕ_{CT} for the $^5D_1 \rightarrow {}^7F_J$ emission are presented for comparison.
† R. Ballardini, E. Chiorboli, and V. Balzani, Inorg. Chim. Acta, 95 (1984) 323.

The delocalization of the d^1 electron in the polyoxometaloeuropate lattices must be also influenced by the configuration of the Eu-O-M linkage as well as the M-O-M linkage: the photoexcitation into the O→M LMCT bands would allow the hopping of the d^1 electron to the EuO_8 or EuO_9 site via two-co-ordinate oxygen 2p orbitals, if the Eu-O-M bond angles are about 150°, since fπ-pπ-dπ orbital mixing on the Eu-O-M linkage would occur with a mode similar to the dπ-pπ-dπ orbital mixing for the corner-sharing MO_6 octahedra with M-O-M bond angles of about 150°. The significance of the Eu-O-M bond angle rationalizes a strong dependence of ϕ_{CT} on the temperature for (3) and (4) with the Eu-O-Mo bond angles of about 150° (Table 2), where the polyoxomolybdate ligands consist of the edge-sharing MoO_6 octahedra with the Mo-O-Mo bond angles of 95-111° [7,8]. Thus, the thermal deactivation channel for the intramolecular energy transfer is the hopping of the d^1 electron over the polyoxometaloeuropate lattice which occurs at both Eu-O-M and M-O-M linkages with the bond angles of about 150° [8]. The small dependence of ϕ_{CT} on the temperature for (1) implies a small extent of the orbital mixing on the Eu-O-W linkage with the Eu-O-W bond angle of about 130° (Table 2). This contrasts with the case for the Eu-O-M bond angle of about 150°.

τ_{CT} for the $^5D_0 \rightarrow {}^7F_J$ emission exhibits a small dependence on the temperature and decreases with an increase in the number (n) of the aqua ligand ((1)>(2)>(3)>(4)). On the other hand, τ_{CT} for the $^5D_1 \rightarrow {}^7F_J$ emission increases with decreasing temperature and exhibits no significant difference among complexes (as τ_{CT} for (3) and (4) at 77K are 11 and 12 μs, respectively). Therefore, the decrease in τ_{CT} for the $^5D_0 \rightarrow {}^7F_J$ emission with an increase in n can be associated with the radiationless deactivation of the $^5D_0$ state due to the weak vibronic coupling with the vibrational states of the high-frequency OH oscillators of the aqua ligand. The decrease in ϕ_{CT} with an increase in n supports this conclusion.

From values of ϕ_{CT} and τ_{CT} at 4.2K, where the intramolecular energy transfer from the O→M LMCT excited states to Eu^{3+} will occur efficiently, the rate of the radiative transition from the $^5D_0$ state can be estimated to be at the range of 2-5 $x10^2$ ($=\phi_{CT}/\tau_{CT}$) s^{-1} for square antiprismatic and tricapped-trigonal prismatic co-ordinations.

3.3 Electroluminescence

The powder-typed EL cell based on the $[EuW_{10}O_{36}]^{9-}$ system exhibits the uniform red EL, when the voltage pulse of -0.8 ~ -1.2 kV with the pulse-width of 0.5-50 ms and with the

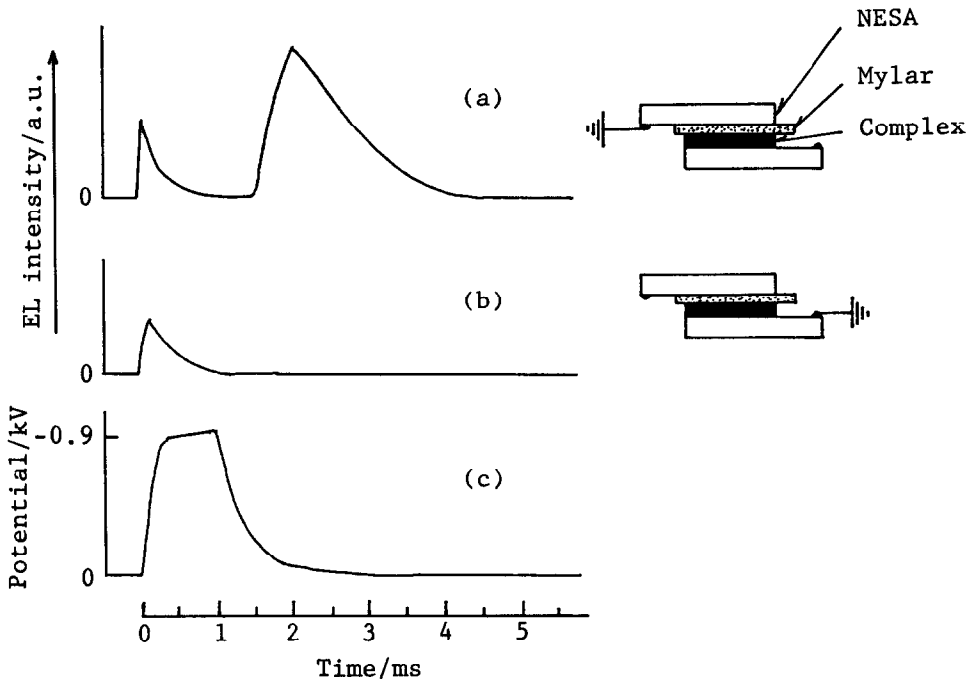

Figure 4. EL transients (a and b) of the $^5D_0 \rightarrow {}^7F_2$ transition at 620 nm for the applied pulse voltage (c).

frequency of 10-500 Hz is applied to the cell consisting of the Ca^{2+} salt layer (about 40 μm thickness) and the insulating Mylar film (6 μm thickness).

The EL spectrum of Eu^{3+} matches the photoluminescence spectrum obtained by the O→W LMCT or Eu^{3+} f-f transition excitation for $[EuW_{10}O_{36}]^{9-}$ in the layer. EL onsets are at the range of -0.6 ~ -0.7 kV and EL intensity increases superlinearly with the applied voltage to -1.2 kV. As the thickness of the insulating Mylar film or the $[EuW_{10}O_{36}]^{9-}$ layer increases, the EL onset voltage shifts toward higher electric field. Figure 4 shows time transients of EL due to the $^5D_0 \rightarrow {}^7F_2$ transition, resulting from the applied pulse step from 0 to -0.90 kV with 1 ms duration and 160 Hz frequency. A peak for the Eu^{3+} emission appears immediately after beginning of the voltage step, and decays to low intensities. When the negative voltage is applied to the $[EuW_{10}O_{36}]^{9-}$-layer-deposited ITO electrode, the Eu^{3+} luminescence appears again after the negative applied pulse is turned off. On the other hand, when the negative voltage pulse was applied to the counter ITO electrode contact with the Mylar film, the second Eu^{3+} luminescence was hardly observed.

An applied external electric field will cause carriers to be injected from the ITO electrode into the $[EuW_{10}O_{36}]^{9-}$-layer, although the direct measurement of the conduction current of such a capacitive device is very difficult due to a large ratio of the displacement current in the load current. Such charge carriers are accelerated to excite the luminescence centers and located finally near the $[EuW_{10}O_{36}]^{9-}$/Mylar interface through which carriers will not be conducted readily, when the negative pulses are applied to the $[EuW_{10}O_{36}]^{9-}$-layer-deposited ITO electrode. Thus, the second Eu^{3+} luminescence occurs only when the conduction charge, accumulated in the vicinity of the $[EuW_{10}O_{36}]^{9-}$/Mylar interface, flows back inside the $[EuW_{10}O_{36}]^{9-}$/ITO electrode interface after the negative applied pulse was turned off.

The polyoxometalate-based EL cell allows the response to a square wave of alternating-polarity pulse, as expected from the above exposition of the data.

4. REFERENCES

1 M.J. Stillman and A.J. Thompson, J. Chem. Soc., Dalton Trans., (1976) 1138.
2 G. Blasse, G.J. Dirksen, and F. Zonnerijlle, J. Inorg. Nucl. Chem., 43 (1981) 2847.
3 R. Ballardini, Q.G. Mulazzani, M. Venturi, F. Bolletta, and V. Balzani, Inorg. Chem., 23 (1984) 300.
4 R. Ballardini, E. Chiorboli, and V. Balzani, Inorg. Chim. Acta, 95 (1984) 323.
5 T. Yamase, H. Naruke, and Y. Sasaki, J. Chem. Soc., Dalton Trans., (1990) 1687.
6 M. Sugeta and Y. Yamase, paper in preparation.
7 H. Naruke, T. Ozeki, and T. Yamase, Acta Crystallogr., C47 (1991) 489.
8 T. Yamase and H. Naruke, J. Chem. Soc., Dalton Trans., (1991) 285.